Design of Differentially-Driven Microstrip Antennas

Y. P. Zhang
School of EEE, Nanyang Technological University
Nanyang Avenue, Singapore, eypzhang@ntu.edu.sg

Abstract

This paper presents the design and experiment on differentially-driven microstrip antennas. First, the design formulas to determine the patch dimensions and the location of the feed point for single-ended microstrip antennas are examined to design differentially-driven microstrip antennas. It is found that the patch length can still be designed using the formulas for the required resonant frequency but the patch width calculated by the formula usually needs to be widen to ensure the excitation of the fundamental mode using the probe feeds. The condition that links the patch width, the locations of the probe feeds, and the excitation of the fundamental mode is given. Both differentially-driven and single-ended microstrip antennas were fabricated and measured. It is shown that the simulated and measured results are in acceptable agreement. More importantly, it is also shown that the differentially-driven microstrip antenna has wider impedance bandwidth of measured 4.1% and simulated 3.9% and higher gain of measured 4.2 dBi and simulated 3.7 dBi as compared with those of measured 1.9% and simulated 1.3% and gain of measured 1.2 dBi and simulated 1.2 dBi of the single-ended microstrip antenna.

1. INTRODUCTION

Microstrip antennas have many unique and attractive properties – low in profile, light in weight, compact and conformable in structure, and easy to fabricate and to be integrated with solid-state devices [1]. Therefore, they have been widely used in radio systems for various applications. Radio systems have been traditionally designed for single-ended signal operation, so have been microstrip antennas. Recently, radio systems have begun to be designed for differential signal operation [2]. This is because the differential signal operation is more suitable for high-level integration or single-chip solution of radio systems. Radio systems that adopt differential signal operation require differential antennas to get rid of bulky off-chip and lossy on-chip balun to improve the receiver noise performance and transmitter power efficiency [3]. There have been a few papers about differential microstrip antennas [4-8]. They focus on either integration with solid-state circuits or analysis of differential signal operation and indeed provide little information on the design of differential microstrip antennas.

In this paper we present the design and experiment on differentially-driven microstrip antennas. We examine the applicability of the design formula and the wideband techniques of single-ended microstrip antennas for differentially-driven microstrip antennas in Section 2. We describe the experiment and discuss the measured results to validate the designs in Section 3. Finally, we summarize the conclusions in Section 4.

2. DESIGN PROCEDURE

A microstrip antenna and a coordinate system are illustrated in Fig. 1. The microstrip antenna that has the patch width a along x-axis and the patch length b along y-axis located on the surface of a grounded dielectric substrate with thickness t, dielectric constant ε_r, and dielectric loss tangent δ is differentially driven at points (x_1, y_1) and (x_2, y_2). The design of the differentially-driven microstrip antenna is to determine the patch width a and length b and the driving points (x_1, y_1) and (x_2, y_2) necessary to satisfy the input impedance and radiation characteristics with the given information on the substrate.
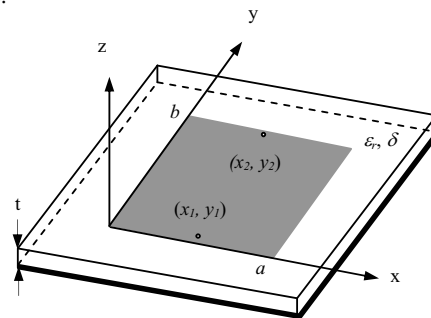

Fig. 1.   Differentially-driven microstrip antenna.

The input impedance Z_d of the differentially-driven microstrip antenna is given by [8]

$$Z_d = 2(Z_{11} - Z_{21}) = 2(Z_{22} - Z_{12}) \qquad (1)$$

where the Z parameters are defined at the driving points (x_1, y_1) and (x_2, y_2) and they can be easily calculated with the improved cavity model [9]. Equation (1) reveals that there is a cancellation mechanism, which may improve the impedance

bandwidth. The value of Z_d is required in the design of matching network between the differentially-driven microstrip antenna and the differential active circuitry in a radio system. The S_{11} calculated from Z_d is given by

$$S_{11} = \frac{Z_d - Z_c}{Z_d + Z_c} \qquad (2)$$

where Z_c is 100 Ω.

For a single-ended microstrip antenna, the patch width a and length b that support the operation at the required resonant frequency (or the free-space wavelength λ_o) can be designed using the formulas as given in [10] as

$$a = \frac{\lambda_o}{2\sqrt{\dfrac{\varepsilon_r + 1}{2}}}, \qquad (3)$$

$$b = \frac{\lambda_o}{2\sqrt{\varepsilon_e}} - 2\Delta b \qquad (4)$$

where

$$\Delta b = 0.412t \frac{\left(\varepsilon_e + 0.3\right)\left(\dfrac{a}{t} + 0.264\right)}{\left(\varepsilon_e - 0.258\right)\left(\dfrac{a}{t} + 0.8\right)}, \qquad (5)$$

$$\varepsilon_e = \frac{\varepsilon_r + 1}{2} + \frac{\varepsilon_r - 1}{2\sqrt{1 + 12\dfrac{t}{a}}}. \qquad (6)$$

The location of the driving point at (x_1, y_1) for matching to 50 Ω can be determined as

$$x_1 = \frac{a}{2}, \qquad (7)$$

$$y_1 = \frac{b}{\pi} \cos^{-1} \frac{a\sqrt{5(\varepsilon_r - 1)}}{3\varepsilon_r b} \qquad (8)$$

where $0 \leq y_1 < b/2$ [11].

While for a differentially-driven microstrip antenna, it is found that the patch length b can still be designed using formulas (3) to (8) for the required resonant frequency. However, the patch width a calculated by formula (3) usually needs to be widen to ensure the excitation of the fundamental mode TM_{01} using the probe feeds. It is known that the larger the patch width is, the higher the radiation efficiency is. The limiting factor for the patch width is the undesirable influence of higher-order modes. For the differentially-driven microstrip antenna, higher-order modes are significantly suppressed. Hence, the patch width for the differentially-driven microstrip antenna can be much larger than that of the single-ended counterpart. The appropriate patch width a for

practical use can be determined together with the location of the driving point (x_2, y_2) for the differentially-driven microstrip antenna. It is natural to locate the driving point (x_2, y_2) at the mirror point of (x_1, y_1) along the line $x = a/2$ within the patch. The condition for the excitation of the fundamental mode TM_{01} using the probe feeds depends on the ratio of the separation to the free-space wavelength, which is given in [8] as

$$\frac{\xi}{\lambda_o} = \frac{y_2 - y_1}{\lambda_o} \geq 0.1 \qquad (9)$$

for an electrically thin substrate. Thus, the patch width for the differentially-driven microstrip antenna can be determined by widening the width calculated from formula (3) to that at which the condition (9) is satisfied. Design using formulas (3) to (9) on the FR4 substrate with $t = 1.6$ mm, $\varepsilon_r = 4.4$, and $\delta = 0.025$ at 2 GHz yields $a = 74.4$ mm, $b = 35$ mm, $(x_1, y_1) = (a/2, 9.654$ mm$)$, and $(x_2, y_2) = (a/2, 25.346$ mm$)$ for the differentially-driven microstrip antenna. The condition $\xi/\lambda_o = 15.692/150 = 0.105 > 0.1$ is satisfied.

3. EXPERIMENT VALIDATION

Both differentially-driven and single-ended microstrip antennas were constructed on the FR4 substrate for operating at 2 GHz. They had the same patch dimensions with nominal values $a = 74.4$ mm and $b = 35$ mm on the ground plane of size 150 mm $\times$ 150mm. The driving points were located at $(x_1, y_1) = (a/2, 9.654$ mm$)$, and $(x_2, y_2) = (a/2, 25.346$ mm$)$ for the differentially-driven microstrip antenna and at $(x_1, y_1) = (a/2, 9.654$ mm$)$ for the single-ended microstrip antenna. An Agilent network analyzer E5062A was used to measure the S_{11}, an HP 8510C network analyzer the radiation patterns, and an Agilent signal generator 8048D and an HP spectrum analyzer 8595E the gain in an NTU anechoic chamber. Due to the lack of facilities to truly measure a differentially-driven antenna, the differentially-driven antenna is conventionally measured by using a balun that forces opposite currents in each feed of the antenna. One balun was used for the pattern and two for the gain measurements. The baluns were ZAPDJ-2 from Mini-Circuits. Fig. 2 shows the photo of the differentially-driven microstrip antenna connected with the balun and the single-ended microstrip antenna as well.

Fig. 2. Photo of the differentially-driven and single-ended microstrip antennas.

The post simulations were made using IE3D for S_{11} and radiation patterns, which considered the fabrication tolerance and the measured balun performance. Fig. 3 shows the simulated and measured S_{11} values of both differentially-driven and single-ended microstrip antennas. Both simulated and measured validate the design can yield the accuracy of the resonant frequency with 2%. It is seen that the differentially-driven microstrip antenna has wider impedance bandwidth of measured 81.5 MHz (4.1%) and simulated 77.6 MHz (3.9%) than those of measured 37.8 MHz (1.9%) and simulated 25.8 MHz (1.3%) of the single-ended microstrip antenna. The agreement between the simulated and measured results is in general acceptable. The discrepancy is likely due to soldering and warpage and the experimental error of our measuring system.

Fig. 4 shows the simulated and measured radiation patterns of both differentially-driven and single-ended microstrip antennas at 2 GHz. It is observed that a good agreement is obtained between the simulation and experiment. It is more interesting to note that the differentially-driven microstrip antenna has much better polarization purity than that of single-ended counterpart. This is particularly remarkable in the H-plane.
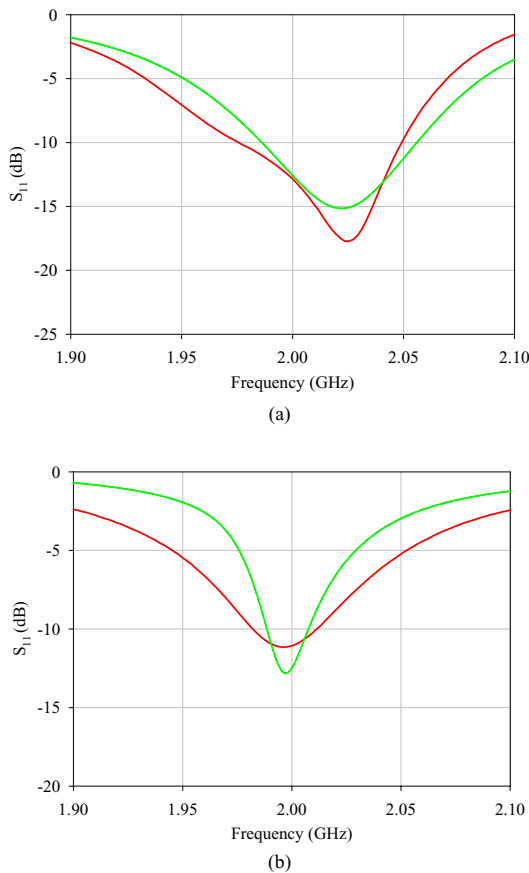
Fig. 3. Simulated and measured S_{11} versus frequency: (a) the differentially-driven antenna and (b) the single-ended microstrip antenna.
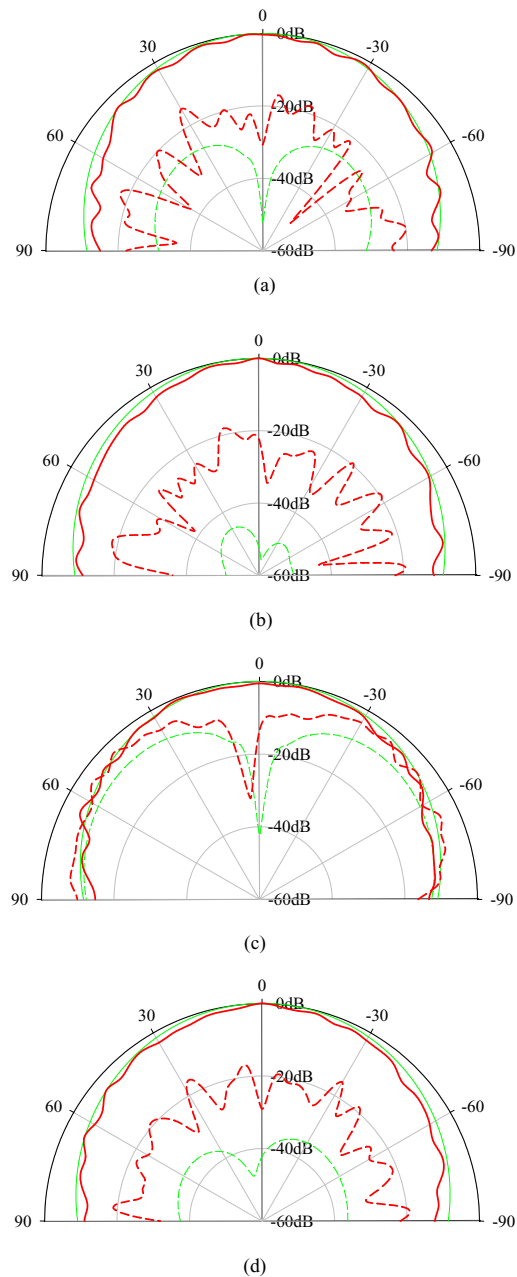

(a)

(b)

(a)

(b)

(c)

(d)

Fig. 4. Simulated and measured radiation patterns at 2.0 GHz: (a) H-plane and (b) E-plane for the differentially-driven antenna and (c) H-plane and (d) E-plane for the single-ended microstrip antenna.

The peak gain was measured with the approach of two identical antennas. The measured peak gain values at 2 GHz are 4.2 and 1.2 dBi for the differentially-driven and single-ended microstrip antennas, respectively. They are quite close

to the simulated peak gain from HFSS values 3.7 dBi for the differentially-driven microstrip antenna and 1.2 dBi for the single-ended microstrip antenna. It is interesting to note that the peak gain values are low, which is mainly due to the large loss tangent associated with the FR4 substrates used. It is more important to note that the peak gain of the differentially-driven microstrip antenna is 3 dB (exactly from the measurements and approximately from the simulations) higher than that of the single-ended microstrip antenna. This is because the differentially-driven microstrip antenna has lower matching loss than that of the single-ended microstrip antenna. Also, the differentially-driven microstrip antenna has significantly suppressed the higher-order TM20 mode; this improves the radiation efficiency of the differentially-driven microstrip antenna.

4. CONCLUSION

This paper focused on the design and experiment on differentially-driven microstrip antennas. The design procedure for differentially-driven microstrip antennas was established for the first time. The computer-aided design formulas to determine the patch dimensions and the location of the feed point for single-ended microstrip antennas were examined for differentially-driven microstrip antennas. It was found that the patch length can still be designed using the formulas for the required resonant frequency but the patch width calculated by the formula usually needs to be widen to ensure the excitation of the fundamental mode using the probe feeds. The condition that links the patch width, the locations of the probe feeds, and the excitation of the fundamental mode was given. Both differentially-driven and single-ended microstrip antennas were fabricated and measured. They validated the design.

REFERENCES

[1] Y. T. Lo, D. Solomon, W. F. Richards, "Theory and experiment on microstrip antennas," *IEEE Trans. Antennas and Propagat.*, vol. 27, no. 2, pp. 137-145, 1979.

[2] A. R. Behzad, M. S. Zhong, S. B. Anand, L. Li, K. A. Carter, M. S. Kappes, T. H. Lin, T. Nguyen, D. Yuan, S. Wu, Y. C. Wong, V. Gong, A. Rofougaran, "A 5-GHz direct-conversion CMOS transceiver utilizing automatic frequency control for the IEEE 802.11a wireless LAN standard," *IEEE J. of Solid-State Circuits*, vol. 38, no. 12, pp. 2209-2220, 2003.

[3] Y. P. Zhang, Development of ICPA in LTCC for single-chip CMOS RF transceivers, NTU Technical Report, 2003

[4] W. R. Deal, V. Radisic, Y. X. Qian, T. Itoh, "Integrated-antenna push-pull power amplifiers," *IEEE Trans. Microwave Theory Tech.*, vol. 47, no. 8, pp. 1418-1425, 1999.

[5] W. Wong, Y. P. Zhang, "0.18-μm CMOS push-pull power amplifier with antenna in IC package," *IEEE Microwave Wireless Comp. Lett.*, vol. 14, no. 1, pp. 13-15, 2004.

[6] P. Abele, E. Ojefors, K. B. Schad, E. Sonmez, A. Trasser, J. Konle, H. Schumacher, "Wafer level integration of a 24 GHz differential SiGe-MMIC oscillator with a patch antenna using BCB as a dielectric layer," *11th GAAS Symposium*, pp. 419-422, Munich 2003.

[7] T. Brauner, R. Vogt, W. Bachtold, "A differential active patch antenna element for array applications," *IEEE Microwave Wireless Comp. Lett.*, vol. 13, no. 4, pp. 161-163, 2003.

[8] Y. P. Zhang, J. J. Wang, "Theory and analysis of differentially-driven microstrip antennas," *IEEE Trans. Antennas and Propagat.*, vol. 54, no. 4, pp. 1092-1099, 2006.

[9] W. F. Richards, Y. T. Lo, D. D. Harrison, "An improved theory for microstrip antennas and applications," *IEEE Trans. Antennas and Propagat.*, vol. 29, no. 1, pp. 38-46, 1981.

[10] K. Hirasawa, *Analysis, Design, and Measurement of Small and Low-Profile Antennas*, Chapter 4. Artech House, 1991.

[11] W. L. Stustzman, G. A. Thiele, *Antenna Theory and Design*, Chapter 5. Wiley, 1998.